Polymer optical fiber tapering without the use of external heat source and its application to refractive index sensing

Hiroki Ujihara, Neisei Hayashi, Kazunari Minakawa, Marie Tabaru, Yosuke Mizuno, and Kentaro Nakamura

Precision and Intelligence Laboratory, Tokyo Institute of Technology, Yokohama 226-8503, Japan

We perform a pilot trial of the highly convenient taper fabrication of perfluorinated graded-index polymer optical fibers. Instead of conventional external heating, we utilize internal heating caused by high-power propagating light (500 mW in this experiment). An approximately 4-mm-long section of a polymer fiber is tapered, and the outer diameter of the ~2-mm-long waist around its midpoint is approximately 200 µm, which is quite uniform with a standard deviation of 4.3 µm. The polymer fiber taper fabricated by this technique is shown to be capable of generating evanescent waves and thus measuring the refractive indices of liquids from 1.333 to 1.410. © 2015 The Japan Society of Applied Physics

The use of Brillouin scattering in optical fibers[1] has unleashed a wide range of applications, such as lasers, signal processors, optical storages, phase conjugators, slow light generators, and strain/temperature sensors.[1–6] To improve their performance, the Brillouin properties of various special glass fibers, which are well summarized in Ref. 7, have been investigated. However, these glass fibers are fragile and must be treated with care; besides, they cannot be used to measure large strains of >3%. One method for overcoming these problems is to employ polymer optical fibers (POFs) with considerable flexibility. POFs can reportedly withstand up to ~100% strain.[8]

Commercially available POFs are classified into two types: poly(methyl methacrylate)-based (PMMA-) step-index POFs[9] and perfluorinated graded-index (PFGI-) POFs[10] based on a cyclic transparent optical polymer (CYTOP®). The former mainly transmits visible light at around 650 nm, whereas the latter transmits not only visible light but also telecom-wavelength light at up to 1.55 µm. Brillouin scattering in PMMA-POFs has not been experimentally observed yet because some of the optical devices required for the measurement are extremely difficult to prepare at visible wavelengths. On the other hand, Brillouin scattering in PFGI-POFs has already been experimentally observed, since various optical devices are available at telecom wavelengths.[11] Their fundamental Brillouin properties, including the Brillouin gain coefficient,[11] Brillouin threshold power,[11] Brillouin frequency shift (BFS),[11] and BFS dependences on strain (relatively small strain[12] and large strain[13]) and temperature,[12] have been investigated at 1.55 µm, especially for sensing applications. These results indicate that Brillouin scattering in PFGI-POFs could be used to develop high-sensitivity temperature sensors[12] and large-strain sensors.[13] The Brillouin Stokes power of PFGI-POFs is, however, typically low because of their large core diameters (50, 62.5, and 120 µm),[11] and must be enhanced both for a more detailed investigation of their Brillouin gain spectra[14–16] and for sensor implementation with a high signal-to-noise ratio.[2–6,17]

The highest optical power that can be injected into POFs is much lower than that of silica single-mode fibers (SMFs) because of the low threshold power of the optical fiber fuse in PFGI-POFs (several hundreds of milliwatts for fuse propagation; much higher power is generally required for fuse ignition).[18,19] Therefore, several methods have been developed to enhance the Stokes signal in PFGI-POFs. One method is to induce stimulated Brillouin scattering using a pump–probe technique, with which an extremely large Stokes signal was obtained in PFGI-POFs.[20] Another method is to use pulsed pump light and a low-power erbium-doped fiber amplifier (EDFA), exploiting the non-linearity of Brillouin scattering.[21] We anticipate that the use of tapered PFGI-POFs is also one of the promising methods for enhancing the Brillouin signal (generated at the tapered section), as the optical power is more concentrated at the core center.[22]

The so-called heat-and-pull technique is most commonly used to taper optical fibers, and has been applied not only to glass fibers[23–29] but also to PMMA-POFs[30,31] and PFGI-POFs.[22,32–34] However, external heat sources, such as a flame,[22–26] a CO_2 laser,[27] a compact furnace,[28,30–33] a solder gun,[34] and a fusion splicer,[29] must be prepared, leading to handling difficulty and/or inconvenience. A chemical etching technique is also used to taper optical fibers,[35] but the use of chemicals impairs convenience. In addition, it is not effective in tapering PFGI-POFs because of the high chemical tolerance of their core material (CYTOP).[10] A more convenient taper fabrication technique of PFGI-POFs is thus required.

In this study, as a pilot trial, we fabricate a PFGI-POF taper by exploiting the internal heating caused by high-power propagating light without the use of an external heat source. We also experimentally show that this PFGI-POF taper can be used to measure the refractive index of liquids.

The PFGI-POF (Asahi Glass Fontex) tapered in this experiment has a three-layered structure consisting of the core (50 µm diameter), and cladding (70 µm diameter) and over-cladding (490 µm diameter) layers. The core and cladding layer are composed of doped and undoped polyperfluoro-butenylvinyl ether, respectively. The refractive index at the center of the core is 1.356, and that of the cladding layer is 1.342. The polycarbonate overcladding layer reduces bending losses and enhances the load-bearing capacity. The propagation loss is relatively low (~250 dB/km), even at 1.55 µm.

The experimental setup used is depicted in Fig. 1. The output of a laser diode at 1552 nm was amplified with an EDFA and injected into a 200-mm-long PFGI-POF. The transmitted power was monitored using an optical power meter. Both ends of the PFGI-POF were butt-coupled to silica SMFs.[11] First, by pressing one point of the PFGI-POF using a nipper, a loss was artificially induced, which was measured to be ~23 dB [optimal value for the incident power of 27 dBm (= 500 mW)]. Subsequently, using motorized stages, the whole length of the PFGI-POF was stretched at a rate of 500 µm/s. The room temperature was 18 °C.
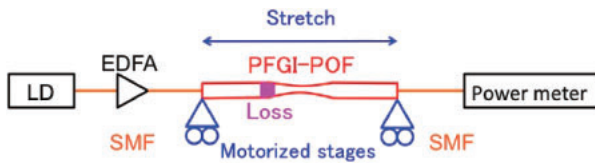
Fig. 1. Schematic of the experimental setup for PFGI-POF tapering. EDFA, erbium-doped fiber amplifier; LD, laser diode; PFGI-POF, perfluorinated graded-index polymer optical fiber; SMF, single-mode fiber.

Fig. 3. Micrograph of the tapered PFGI-POF.
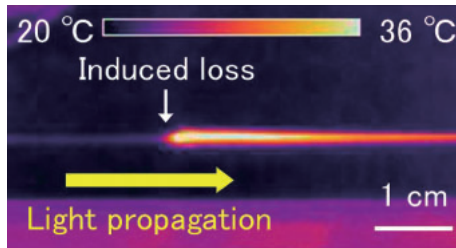
Fig. 2. Thermograph around the loss-induced point in the PFGI-POF.

Fig. 4. Outer diameter distribution around the waist of the PFGI-POF taper.

First, the PFGI-POF section around the artificially induced loss was monitored using an infrared thermometer,[36] as shown in Fig. 2. The incident light, the power of which was set to 27 dBm, was injected from the left-hand side. This power is higher than the threshold for fiber fuse propagation,[18,19] but generally lower than the threshold for fuse ignition; the fuse was never ignited in this tapering experiment (in Refs. 18 and 19, a POF end was brought into contact with an absorbent material to ignite the fuse). The high-temperature region had a tail extending for ∼5 cm toward the right. This seems to originate from the fact that the optical paths of the propagating rays were partially disturbed at the loss, and that the optical energy was then absorbed by the overcladding layer located slightly away from the loss, generating heat as a result. The maximal temperature of the color bar in Fig. 2 is 36 °C, which is much lower than the glass transition temperature of the core material (approximately 100 °C) for the following two reasons: (1) 36 °C is not the temperature at the hottest point that is initially tapered but that at the center of the infrared image (owing to the specifications of the camera) and (2) the temperature measured by this method is the surface temperature of the overcladding layer of the POF, which is lower than the core temperature.

Next, while maintaining the incident light power (27 dBm), the loss-induced PFGI-POF was stretched for 4 mm. Then, as shown in Fig. 3, taper deformation started rightward from the point ∼1 mm away from the induced loss. The distribution of the outer diameter along the length measured with an optical microscope is shown in Fig. 4. An approximately 4-mm-long section was tapered, and the outer diameter of the ∼2-mm-long waist around its midpoint was approximately 200 µm, which was quite uniform with a standard deviation of 4.3 µm. Such a high uniformity seems to have been achieved by the yielding of the overcladding layer made of polycarbonate (see Refs. 37 and 38). The outer diameters at the relative positions of 0 and 6 mm (see Fig. 4) were ∼40 and ∼90 µm smaller than the initial outer diameter (490 µm), respectively. This is because the nontapered regions were also slightly stretched, which is clear if we consider that the fabricated
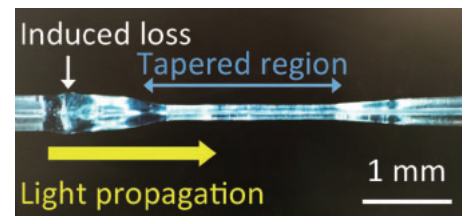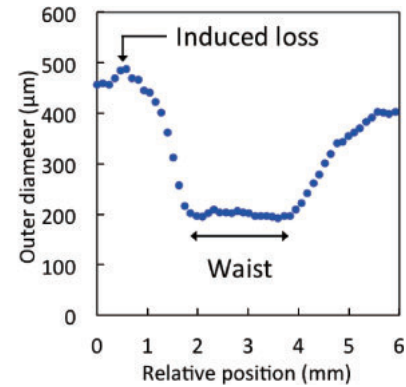
taper length is almost the same as the stretched length (∼4 mm). The deformation on the right (relative position of 6 mm in Fig. 4) was larger probably because the temperature was higher (see Fig. 2). Thus, the structural asymmetry in the axial direction is inevitable in this method, and may present a problem with some applications. The propagation loss of this taper, excluding the initially induced ∼23 dB loss, was measured to be ∼25 dB.

To verify the refractive index sensing capability on the basis of evanescent wave generation,[32–34,39–41] the whole length (∼4 mm) of the tapered PFGI-POF section was placed in a V-groove (machined flat to minimize fiber bending) and immersed in sucrose solutions with different concentrations. Sucrose concentrations of 0.0, 12.0, 24.0, 35.0, and 45.0% were employed, corresponding to the refractive indices of 1.333, 1.351, 1.371, 1.390, and 1.410, respectively.[42] The PFGI-POF taper and the V-groove were carefully cleaned, washed with ethanol and deionized water, and then dried before the immersion of the taper into the next sucrose solution. In this experiment, light at a power of 10 dBm was injected into the PFGI-POF taper from the same side as in the case of taper fabrication. The transmitted light power was measured in all cases at a constant temperature of 18 °C.

The measured loss dependence on the refractive index of the sucrose solution is shown in Fig. 5. The loss in the vertical axis, calculated relative to the incident power (10 dBm), does not include the initially induced ∼23-dB loss. As the refractive index increased, the loss almost linearly (though the vertical axis is in the unit of dB) increased in this range with a dependence coefficient of 107 dB/RIU (refractive index unit). Although it is difficult to compare the absolute value directly with those in previous reports measured under different experimental conditions and POF structures,[31,32,34] the positive coefficient of the loss (i.e., negative coefficient of the transmitted power) agrees with that
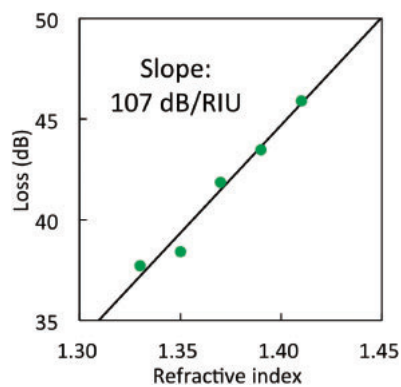
Fig. 5. Optical loss at the taper (excluding the initially induced loss) as a function of the refractive index of liquids. The measured data are shown as green circles, and the black line shows a linear fit.

in the case where the PMMA-POF tapers fabricated using a heat-and-pull technique were tested with a similar setup.[31] When the nontapered regions were immersed into the sucrose solutions, no quantifiable influence was observed on the transmitted power. Thus, we confirmed that the PFGI-POF taper fabricated using internal heating generates the evanescent waves, which is one of the fundamental functions of fiber optic tapers.

In conclusion, we demonstrated PFGI-POF taper fabrication. Without the use of an external heat source, internal heating caused by high-power propagating light was exploited. We showed that the PFGI-POF taper generates evanescent waves that can be used to measure the refractive index of liquids. The initially induced loss, which remains after taper fabrication, is an important issue to be resolved; therefore, the PFGI-POF tapers fabricated by this technique may be more suitable for refractive index sensing with a reflectometry configuration, such as that exploiting tapered fiber tips.[43] The clarification of the controllability of the taper shape characteristics, such as outer diameter and waist length, will certainly be the subject of future work. If long PFGI-POF tapers can be relatively easily fabricated by this technique, we anticipate that it will exert a powerful impact on POF-based Brillouin sensing.

1) G. P. Agrawal, *Nonlinear Fiber Optics* (Academic Press, San Diego, CA, 1995).
2) T. Horiguchi and M. Tateda, J. Lightwave Technol. **7**, 1170 (1989).
3) T. Kurashima, T. Horiguchi, H. Izumita, S. Furukawa, and Y. Koyamada, IEICE Trans. Commun. **E76-B**, 382 (1993).
4) D. Garus, K. Krebber, F. Schliep, and T. Gogolla, Opt. Lett. **21**, 1402 (1996).
5) K. Hotate and T. Hasegawa, IEICE Trans. Electron. **E83-C**, 405 (2000).
6) Y. Mizuno, W. Zou, Z. He, and K. Hotate, Opt. Express **16**, 12148 (2008).
7) Y. Mizuno, N. Hayashi, and K. Nakamura, J. Appl. Phys. **112**, 043109 (2012).
8) H. Ujihara, N. Hayashi, M. Tabaru, Y. Mizuno, and K. Nakamura, IEICE Electron. Express **11**, 20140707 (2014).
9) M. G. Kuzyk, *Polymer Fiber Optics: Materials, Physics, and Applications* (CRC Press, Boca Raton, FL, 2006).
10) Y. Koike and M. Asai, NPG Asia Mater. **1**, 22 (2009).
11) Y. Mizuno and K. Nakamura, Appl. Phys. Lett. **97**, 021103 (2010).
12) Y. Mizuno and K. Nakamura, Opt. Lett. **35**, 3985 (2010).
13) N. Hayashi, Y. Mizuno, and K. Nakamura, Opt. Express **20**, 21101 (2012).
14) A. Yeniay, J. M. Delavaux, and J. Toulouse, J. Lightwave Technol. **20**, 1425 (2002).
15) M. Nikles, L. Thevenaz, and P. A. Robert, J. Lightwave Technol. **15**, 1842 (1997).
16) R. B. Jenkins, R. M. Sova, and R. I. Joseph, J. Lightwave Technol. **25**, 763 (2007).
17) N. Hayashi, Y. Mizuno, and K. Nakamura, J. Lightwave Technol. **32**, 3999 (2014).
18) Y. Mizuno, N. Hayashi, H. Tanaka, K. Nakamura, and S. Todoroki, Appl. Phys. Lett. **104**, 043302 (2014).
19) Y. Mizuno, N. Hayashi, H. Tanaka, K. Nakamura, and S. Todoroki, Sci. Rep. **4**, 4800 (2014).
20) Y. Mizuno, M. Kishi, K. Hotate, T. Ishigure, and K. Nakamura, Opt. Lett. **36**, 2378 (2011).
21) Y. Mizuno and K. Nakamura, Appl. Phys. Express **5**, 032501 (2012).
22) N. Hayashi, H. Fukuda, Y. Mizuno, and K. Nakamura, J. Appl. Phys. **115**, 173108 (2014).
23) J. C. Knight, G. Cheung, F. Jacques, and T. A. Birks, Opt. Lett. **22**, 1129 (1997).
24) T. A. Birks, W. J. Wadsworth, and P. St. J. Russel, Opt. Lett. **25**, 1415 (2000).
25) L. Tong, R. R. Gattass, J. B. Ashcom, S. He, J. Lou, M. Shen, I. Maxwell, and E. Mazur, Nature **426**, 816 (2003).
26) G. Brambilla, V. Finazzi, and D. J. Richardson, Opt. Express **12**, 2258 (2004).
27) T. E. Dimmick, G. Kakarantzas, T. A. Birks, and P. St. J. Russell, Appl. Opt. **38**, 6845 (1999).
28) M. Sumetsky, Y. Dulashko, and A. Hale, Opt. Express **12**, 3521 (2004).
29) F. Lissillour, D. Messager, G. Stéphan, and P. Féron, Opt. Lett. **26**, 1051 (2001).
30) Y. Jeong, S. Bae, and K. Oh, Curr. Appl. Phys. **9**, e273 (2009).
31) D.-J. Feng, G.-X. Liu, X.-L. Liu, M.-S. Jiang, and Q.-M. Sui, Appl. Opt. **53**, 2007 (2014).
32) J. Arrue, F. Jiménez, G. Aldabaldetreku, G. Durana, J. Zubia, M. Lomer, and J. Mateo, Opt. Express **16**, 16616 (2008).
33) R. Gravina, G. Testa, and R. Bernini, Sensors **9**, 10423 (2009).
34) A. A. Jasim, N. Hayashi, S. W. Harun, H. Ahmad, R. Penny, Y. Mizuno, and K. Nakamura, Sens. Actuators A **219**, 94 (2014).
35) D. F. Merchant, P. J. Scully, and N. F. Schmitt, Sens. Actuators A **76**, 365 (1999).
36) N. Hayashi, Y. Mizuno, and K. Nakamura, Appl. Phys. Express **6**, 076601 (2013).
37) S. S. Sarva and M. C. Boyce, J. Mech. Mater. Struct. **2**, 1853 (2007).
38) N. Hayashi, K. Minakawa, Y. Mizuno, and K. Nakamura, Appl. Phys. Lett. **105**, 091113 (2014).
39) P. Wang, G. Brambilla, M. Ding, Y. Semenova, Q. Wu, and G. Farrell, Opt. Lett. **36**, 2233 (2011).
40) C. L. Linslal, P. M. S. Mohan, A. Halder, and T. K. Gangopadhyay, Sens. Actuators A **194**, 160 (2013).
41) A. Leung, K. Rijal, P. M. Shankar, and R. Mutharasan, Biosens. Bioelectron. **21**, 2202 (2006).
42) D. R. Lide, *Handbook of Chemistry and Physics* (CRC Press, Boca Raton, FL, 2004).
43) Y. H. Tai and P. K. Wei, Opt. Lett. **35**, 944 (2010).